Glass Physics and Chemistry, Vol. 31, No. 4, 2005, pp. 535–544.

PROCEEDINGS OF THE TOPICAL MEETING OF THE EUROPEAN CERAMIC SOCIETY "NANOPARTICLES, NANOSTRUCTURES, AND NANOCOMPOSITES"

(St. Petersburg, Russia, July 5–7, 2004)

Tunneling Current–Voltage Controls, Oscillations, and Instability of Nanotube- and Nanowire-Based Nanoelectromechanical Systems[1]

N. Pugno

Department of Structural Engineering, Politecnico di Torino, Corso Duca degli Abruzzi 24, 10129, Torino, Italy

Abstract—In this paper, vibrations, instability, and control of nanotube- and nanowire-based nanoelectromechanical systems (NEMS) are investigated. A dynamic analysis is presented, which includes the role of the electric field, van der Waals forces, temperature, and the uncertainty principle. Furthermore, the system instability, arising at the so-called pull-in voltage and corresponding to the on–off transition of the device, is also quantified. Active current and voltage controls based on the quantum tunneling effect are discussed. It is shown that the tunneling current between the cantilever nanotube/nanowire tip and the electrode substrate would correspond to the realization of an analogic device (e.g., nanotweezers) if the current is in control or to a digital device (e.g., nanoswitch) if the voltage is controlled. Finally, the characteristic electromechanical curves voltage/current–displacement for the NEMS are deduced.

INTRODUCTION

Carbon nanotubes (CNTs) are attracting significant attention because of their unique mechanical and electronic properties. Consequently, CNTs are considered to be ideal building blocks for nanoelectromechanical systems (NEMS) devices. By exploiting nanoscale effects, NEMS also present interesting and unique characteristics. For instance, CNT-based NEMS devices can have an extremely high fundamental frequency [1–4] and preserve very high mechanical responsivity [5]. Several NEMS devices have been reported, such as mass sensors and radiofrequency (RF) resonators [6], field-effect transistors (FET) [7], and electrometers [8]. CNT-based NEMS devices reported in the literature include nanotweezers [9, 10], nonvolatile random access memory (RAM) [11], nanorelays [12], and rotational actuators [13].

NEMS seem to have the capability to revolutionize the electronic components of the future. Their tremendously miniaturized size and high fundamental frequency would result in a density of the order of 10^{12} elements over a square centimeter and an operation frequency in the EHF band (extrahigh frequency, 30–300 GHz).

Regarding the prediction of the mechanical strength of nanostructures, a new theory, namely, quantized fracture mechanics (QFM), has recently been developed [14]. QFM seems to be have been confirmed by experimental results and atomic–quantum mechanical numerical analyses on nanostructures, e.g., on defective nanotubes. Fracture of tiny systems with a given geometry and type of loading occurs at "quantized" stress levels that are predicted well by QFM. Such investigations confirm that nanotubes and nanowires remain the key elements for designing innovative NEMS, due to their tremendous mechanical properties.

Assuming a sufficient mechanical strength, the dynamics, switch, and controls of NEMS, always oscillating (at least as a consequence of the thermal vibrations), represent still open and fundamental issues in an optimal design. Such vibrations are usually studied assuming a linear behavior and without considering the effect of the electric and van der Waals fields imposed to control the device. In spite of this, the presence of electrostatic charges implies that the nanotube/nanowire cannot be considered as free, as is usually assumed. Moreover, linear behavior, implicitly corresponding to the assumption of small displacements, seems to be in contrast with the observed high flexibility of nanotubes (and nanowires), which are capable of undergoing large displacements while remaining in the elastic regime. In this paper, we try to remove these assumptions. The static equilibrium configuration of the NEMS is derived by minimizing its free energy. The oscillations around such a configuration are studied, and the equipartition theorem is applied to study the thermal vibrations. An experimental comparison is discussed. Moreover, the amplitude of the intrinsic oscillations at a temperature of 0 K, as imposed by the uncertainty principle, is also estimated. The intensity of the electric field corresponding to a vanishing oscillating frequency (i.e., to a structural instability) is predicted for nanotube- and nanowire-based NEMS and compared with numerical

[1] This article was submitted by the author in English.

1087-6596/05/3104-0535

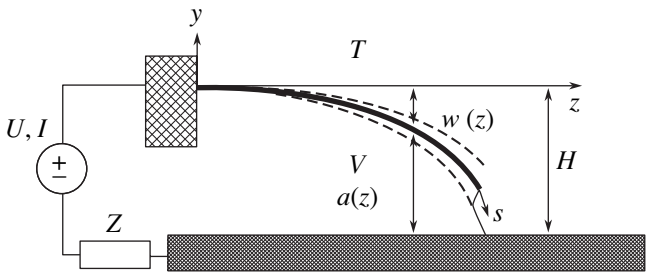

Fig. 1. Current and voltage controlled nanotube/nanowire cantilever vibrating NEMS.

simulations. Such a prediction of the pull-in voltage is shown to be fundamental, since it represents the key design parameter describing the on–off transition of the device [15, 16].

Moreover, the control of a CNT-based cantilever NEMS device is extensively investigated. Similar considerations could be proposed for nanowires. The device, i.e., the clamped nanotube suspended over the electrode, is assumed to be in series with an impedance *Z*. In the analysis, we will focus our attention on a pure resistance, as was numerically investigated in [17, 18]. The system can be controlled by imposing a current *I* or a voltage *U* from an electrical power supply that we assume to be ideal. A current between the nanotube tip and the ground electrode (from which a difference *V* in the potential exists) will take place in the circuit for small gaps (on the order of 1 nm) as a consequence of the tunneling effect (with associated tunneling resistance R_T) [19–21]. The device is depicted in Fig. 1. If the power supply imposes a current (pA range), the nanotube will be deflected towards the electrode, eventually reaching a given tip position corresponding to a tunneling current between the tip and the electrode as imposed by the power supply; thus, an ideal current control results in an analogic device. The impedance *Z* in this case does not possess any particular role and can be neglected. Assuming a zero impedance, in the circuit (Fig. 1) $U = V$, the nanotube will collapse onto the electrode at a given pull-in voltage $U = U_{PI}$ [22]. When the applied voltage $U < U_{PI}$, the elastic force of the CNT is balanced by the electrostatic force. The cantilever CNT remains in the upper equilibrium position. Here, the deflection is controlled by the applied voltage. When the pull-in voltage is exceeded, the system becomes unstable, and, without any increase in the applied voltage *U*, the electrostatic force becomes larger than the elastic force and the CNT collapses onto the bottom electrode. After the pull-in, due to the van der Waals forces, the sticking of the device, also removing the applied voltage, in general remains (if the elastic forces are larger than the van der Waals forces, the nanotube recovers its undeformed configuration). Thus, a pure voltage control results in a onetime switchable device; note that, for some applications, this could be a desired effect. The impedance *Z* in the circuit allows this (in general, negative) effect to be avoided, as numerically investigated for the case of pure resistive impedance in [17, 18]. When the tip of the CNT is very close to the electrode, as shown in Fig. 1 (i.e., a distance of around 1 nm), a substantial tunneling current takes place between the tip of the CNT and the bottom electrode. Due to the existence of the resistive impedance *Z* in the circuit, the postcritical (after the pull-in) behavior changes radically with respect to the case of zero impedance. The voltage *V* applied to the CNT drops as a consequence of the tunneling current, weakening the electric field. Consequently, the nanotube moves towards a second equilibrium position due to the presence of damping in the real system. At this point, if the applied voltage *U* decreases, the CNT cantilever starts retracting. When *U* decreases to a certain value, the so-called pull-out voltage U_{PO}, the CNT cantilever is released from its lower equilibrium position and returns to its upper equilibrium position [17, 18]. Thus, this voltage control, with a feedback resistive impedance, corresponds to a switchable bistable device. However, in this case, the system needs a power consumption to maintain the on position, in contrast to the nondissipative solution proposed in [11].

In this paper, we try to quantify the qualitatively described NEMS behaviors.

NEMS OSCILLATIONS AND INSTABILITY

Let us focus our attention on a cantilever clamped nanotube (cylindrical cross section) or nanowire (rectangular cross section) suspended over an electrode at a distance *H* from which a difference *V* in the electrostatic potential is imposed by a voltage *U* or a current *I* supply; the system is vibrating at a given temperature *T* (Fig. 1). Let us start by considering a vanishing impedance *Z* in the circuit and voltage control, so that $U = V$.

The electrostatic $\varepsilon_{\text{elec}}$ and van der Waals ε_{vdW} energies per unit length can be evaluated by the following relationships [22]:

$$\frac{d\varepsilon_{\text{elec}}}{ds} = \frac{\pi\varepsilon_0 V^2}{\cosh^{-1}\left(1+\frac{a}{r}\right)}, \text{ nanotube} \quad (1)$$

$$\frac{d\varepsilon_{vdW}}{ds} = \sum_{r=r_{\text{int}}}^{r_{\text{ext}}}\sum_{a=a_{\text{int}}}^{a_{\text{int}}+(N_G-1)d} \frac{\pi^2 C_6 n^2 d^2 r(a+r)(3r^2+2(a+r)^2)}{2((a+r)^2-r^2)^{7/2}}, \quad (2)$$

nanotube

$$\frac{d\varepsilon_{\text{elec}}}{ds} = \frac{B}{2}\varepsilon_0\frac{V^2}{a}, \quad \text{nanowire} \quad (3)$$

$$\frac{d\varepsilon_{vdW}}{ds} = \frac{B\pi C_6 n^2}{12}\left(\frac{1}{a^2} - \frac{1}{(a+t)^2}\right), \quad \text{nanowire}, \quad (4)$$

where s is the natural axial coordinate along the deflected configuration (coincident with the horizontal coordinate z only for small displacements), r_{int} and $r \equiv r_{\text{ext}}$ are the inner and outer radius of a (multiwalled) nanotube, N_G is the number of layers in the substrate (usually graphite), d is the interlayer distance (for graphite, $d = 0.335$ nm). In addition, $a \equiv a_{\text{int}}$ is the gap between the nanotube (external wall) and the surface layer of the substrate, where n is the atomic density (for graphite, it is equal to $n = 1.14 \times 10^{29}$ m^{-3}); $\varepsilon_0 = 8.85 \times 10^{-12}$ C^2/(N m^2) is the vacuum permittivity, and C_6 is a material constant (for graphite, it is equal to $C_6 = 2.43 \times 10^{-78}$ Nm^7); for nanowires, B denotes the width (parallel to the substrate) and t is the thickness of the cross-sectional area; $w(z) = H - a(z)$ is the system deflection, and E and J are the Young modulus and the moment of inertia (equal to $\pi(r_{\text{ext}}^4 - r_{\text{int}}^4)/4$ for nanotube or to $Bt^3/12$ for nanowire), respectively. We have assumed a rectangular cross section for the nanowire, but this hypothesis can be easily relaxed.

Let us consider a deformed static configuration w_S assumed as a given arbitrary function satisfying the boundary conditions, with one (or more) unknown free parameter(s) c_S (e.g., $w_S \approx c_S s^2/L^2$, with c_S corresponding to the tip displacement). The oscillations around this configuration can be described by

$$w(s, t) = w_S(s) + w_D(s, t). \quad (5)$$

For the fundamental frequency ω, the function $w_D(s, t)$ will be

$$w_D(s, t) \approx \frac{w_S(s)}{c_S} c_D \sin(\omega t), \quad (6)$$

where c_D represents the maximum amplitude of the harmonic oscillations around the equilibrium position described by c_S (that minimizes the free energy of the system). Accordingly, the kinetic energy of the NEMS will be

$$K(t) = \frac{1}{2}\int_M \left(\frac{dw(s,t)}{dt}\right)^2 dM = \frac{\mu}{2}\int_0^L \left(\frac{dw_D(s,t)}{dt}\right)^2 ds. \quad (7)$$

Here, M is the mass of the nanotube/nanowire and $\mu = \rho_m S$, where S is the cross-sectional area and ρ_m is the density (for carbon, $\rho_m = 2260$ kg/m^3). Equation (7) can be rewritten as

$$K(t) = \frac{1}{2} m_{\text{eq}} c_D^2 \omega^2 \cos^2(\omega t), \quad m_{\text{eq}} = \alpha M, \quad (8)$$

where α is dependent on the chosen form for w_S (e.g., rough forms of w_S give estimations for the cantilever of $\alpha \approx 1/5$) and can be derived by comparing Eqs. (7) and (8).

Indicating the free energy of the NEMS by $W(c)$, where $c = c_S + c_D \sin(\omega t)$, and fixing its reference by imposing $W(c_S) = 0$, by equating the maximum value of the free energy and the maximum kinetic energy, we obtain an estimate of the fundamental (operating) frequency ω as

$$\omega^2 = \frac{2W_{\max}}{m_{\text{eq}} c_D^2}. \quad (9)$$

If the kinetic energy (e.g., its mean value) is a given quantity, from Eqs. (8) and (9), the frequency and the amplitude of the oscillations can be derived. Note that, in general (if the oscillations are large), the frequency ω will be a function also of the amplitude c_D, as described by Eq. (9), showing a nonlinear behavior. For small oscillations, the frequency becomes amplitude-independent, as emphasized in the next section.

Small oscillations. If the oscillations are small (also around a large deflected configuration), we can develop the free energy in series, considering just the two first terms. Since, at the static equilibrium, the free energy must present a minimum, i.e., $\left.\frac{dW(c)}{dc}\right|_{c=c_S} = 0$, as well as $W(c_S) \equiv 0$ (according to the chosen reference system), we have

$$\begin{aligned} W(c) &\cong \frac{1}{2}\left.\frac{d^2W(c)}{dc^2}\right|_{c=c_S} (c - c_S)^2 \\ &= \frac{1}{2}\left.\frac{d^2W(c)}{dc^2}\right|_{c=c_S} (c_D \sin(\omega t))^2 \end{aligned} \quad (10)$$

so that, applying Eq. (9), it follows that

$$\omega^2 = \frac{\left.\frac{d^2W(c)}{dc^2}\right|_{c=c_S}}{m_{\text{eq}}}. \quad (11)$$

Note that, under these assumptions, ω does not depend on the amplitude c_D but only on the external fields included in the free energy term.

Free oscillations. Focusing our attention on free oscillations, the free energy becomes coincident with the elastic energy stored in the nanotube; i.e., $W(c) = \varepsilon_{\text{elast}}(c)$, where

$$\varepsilon_{\text{elast}}(c) = \frac{EJ}{2}\int_0^L \left(\frac{d\theta}{ds}\right)^2 ds = \frac{\beta EJ}{L^3} c^2, \quad (12)$$

where θ defines the slope of the elastic line of the nanotube, i.e., $\theta = dw/dz$, and β is a known coefficient dependent on the chosen form for w_S (e.g., a rough esti-

mation for the cantilever is $\beta \approx 1$). Thus, from Eq. (11),

$$\omega^2 = \frac{2\beta EJ}{L^3 m_{\text{eq}}}. \quad (13)$$

Thermal vibrations. For thermal vibrations at an absolute temperature T, the equipartition theorem implies a known mean value $k_B T/2$ (k_B is Boltzmann's constant) of the kinetic energy associated with each degree of freedom; hence,

$$\langle K(\tau) \rangle = \frac{1}{P}\int_P K(\tau) d\tau = \frac{k_B T}{2}, \quad (14)$$

where $P = 2\pi/\omega$ is the period of the oscillation. Comparison of Eq. (14) with the mean value of Eq. (8), in light of Eq. (11), gives

$$c_D^2 = \frac{2k_B T}{\left.\frac{d^2 W(c)}{dc^2}\right|_{c = c_S}}, \quad (15)$$

from which we can obtain the amplitude c_D of the thermal vibrations around the position described by c_S. The frequency is given by Eq. (11).

The equipartition theorem applied to the higher modes m fixes their relative amplitudes, which fall off as $\sim 1/m^2$. Thus, the first mode $m = 1$ (that we are investigating) is clearly the predominant one.

Free thermal vibrations. Considering the thermal vibrations around the relaxed configuration $W(c) = \varepsilon_{\text{elast}}(c)$ and introducing Eq. (12) into Eq. (15) yields

$$c_D^2 = \frac{L^3 k_B T}{\beta EJ} \quad (16)$$

with ω given by Eq. (13).

Instability. The instability of the system arising at the so-called pull-in voltage, is achieved when the global stiffness of the NEMS becomes negligible, i.e., when the frequency of the oscillations formally goes to zero:

$$\omega^2 = \frac{\left.\frac{d^2 W(c)}{dc^2}\right|_{c = c_S}}{m_{\text{eq}}} = 0. \quad (17)$$

According to Eqs. (11) and (15), the thermal vibrations are predicted to be infinitely large at zero frequency. Practically, when they become large enough, the approximation of small vibrations is no longer valid and the amplitude will be limited. Thus, from the condition of Eq. (17), the pull-in voltage can be easily estimated, as shown below.

The kinetic energy released after the pull-in can be evaluated as

$$K_{PI} \cong W_{PI} - W_{\text{contact}}, \quad (18)$$

where W_{PI} is the free energy at the pull-in and W_{contact} is the free energy after the impact of the nanotube on the electrode, i.e., in the collapsed configuration.

The oscillations imposed by the Heisenberg principle. The Hamiltonian ($\mathcal{H}$) of the NEMS must have the form of ($W(c_S) = 0$)

$$\mathcal{H}(c, t) = K(c, t) + W(c). \quad (19)$$

The Schrödinger equation of the continuum system can be correspondingly written in a simple manner as a consequence of the reduction of the system to one degree of freedom:

$$\left(-\frac{\hbar^2}{2m_{\text{eq}}}\frac{d^2}{dc^2} + W(c)\right)\psi_n(c) = \varepsilon_n \psi_n(c), \quad (20)$$

where ε_n are the energy eigenvalues and ψ_n are the eigenfunctions describing the fundamental vibrational states. Equation (20) can be solved numerically. For small dynamic displacements around a (similarly large) deflected configuration, we can substitute the conditions of Eqs. (10) and (11), thus finding the well-known discrete quantized energy levels of the harmonic oscillator:

$$\varepsilon_n \approx \left(\frac{1}{2} + n\right)\hbar\omega. \quad (21)$$

Note that, here, ω is not the fundamental frequency of the cantilever nanotube/nanowire but, according to Eq. (11), takes into account the external fields, included in the free energy. Obviously, the lowest energy level is predicted to be different from zero also at zero temperature

$$\varepsilon_0 \approx \frac{\hbar\omega}{2}, \quad (22)$$

as imposed by the Heisenberg principle (the total energy is the sum of the potential and kinetic energies, both positively defined; considering $\varepsilon_0 \approx 0$ would imply that both the position and velocity of the system are known (and equal to zero), which contradicts the uncertainty principle). Between two adjacent levels, the energy gap is, as well-known, $\Delta\varepsilon = \varepsilon_{n+1} - \varepsilon_n = \hbar\omega$.

The condition for which Eq. (22) equals Eq. (14) corresponds to the temperature for which the "vibrations" (corresponding to the borderline with the quantum accessibility) at the zero point become larger than the thermal vibrations:

$$k_B T \approx \hbar\omega. \quad (23)$$

Substituting Eq. (23) into Eq. (15) implies considering the energy of Eq. (22) as the mean value of the kinetic energy at 0 K; thus, the amplitude of the "vibrations" at a temperature of 0 K must be of the order of

$$c_D^2 = \frac{L^3 \hbar\omega}{\beta EJ} = \hbar\sqrt{\frac{2L^3}{\beta EJ m_{\text{eq}}}} \quad (24)$$

with a frequency given by Eq. (13).

Free energy of the NEMS. To quantify the approach proposed in the previous sections, it is sufficient to derive an expression for the free energy of the NEMS. This step represents the aim of the present section.

The free energy of the NEMS has to be written as

$$W(c) = \varepsilon_{\text{elast}}(c) - \varepsilon_{\text{elec}}(c) - \varepsilon_{vdW}(c). \quad (25)$$

If the gaps are smaller than a critical value (around 1 nm), the Pauli energy $\varepsilon_{\text{Pauli}}(c)$ (with a minus sign) plays a significant role and has to be added to the right-hand side of Eq. (25). Otherwise, it can be neglected. The elastic energy is given by Eq. (12).

For computing the electrostatic energy, we assume a uniform charge distribution [22].

The total electrostatic and van der Waals energies stored in the NEMS are

$$\varepsilon_{\text{elec}}(c) = \int_0^L \frac{d\varepsilon_{\text{elec}}}{ds} ds, \quad (26)$$

$$\varepsilon_{vdW}(c) = \int_0^L \frac{d\varepsilon_{vdW}}{ds} ds. \quad (27)$$

Thus, the free energy of Eq. (25) is now quantified by Eqs. (1)–(4) and (12), (26), (27); the amplitude and frequency of the oscillations can consequently be evaluated as previously described. Note that, before applying the relationships previously derived, the free energy of Eq. (25) must be rewritten according to our choice of $W(c_S) = 0$, where c_S: $\left.\frac{dW(c)}{dc}\right|_{c=c_S} = 0$. For example, applying Eq. (17), we find the NEMS instability arising at the so-called pull-in voltage for

$$V_{PI} = k\frac{H}{L^2}\ln\left(\frac{2H}{R}\right)\sqrt{\frac{\beta EJ}{\varepsilon_0}}, \quad (28)$$

$$V_{PI} \approx \zeta\sqrt{\frac{\beta Et^3H^3}{\varepsilon_0 L^4}}, \quad (29)$$

where $k \approx 0.85$, $\zeta \approx 1$. Note that, for a clamped–clamped configuration, we estimate $\beta \approx 48$ (even if, for such a configuration, the stretching of the nanotube could play a significant role [23]). Here, we have neglected the van der Waals forces that have to be considered only for gaps (technologically still unrealistic) lower than ~10 nm. However, considering the first corrective term accounting for the van der Waals forces, we find the instability at V_{PI}^{vdW}, with a shift with respect to V_{PI} given (for example, for a nanotube having N_W walls) by

$$\Delta^{vdW}V_{PI} = V_{PI} - V_{PI}^{vdW} \approx 2nd\ln\left(\frac{2H}{r}\right)\sqrt{\frac{C_6HN_W\langle r\rangle\sum_{i=0}^{N_G-1}(H+id)^{-5}}{\varepsilon_0}}. \quad (30)$$

Comparison with experimental and numerical results. Let us focus on nanotubes. Usually, free and thermal vibrations of nanotube-based NEMS are studied around the relaxed configuration, due to the higher complexity in treating the effect of the electric field and van der Waals forces in the dynamics of the system. Neglecting such effects, the classical continuum approach to the study of the free vibrations (even thermal, by virtue of the equipartition theorem) of the beams holds; on the other hand, the proposed approach allows one to estimate the effect of the external fields as well as the "vibrations" at a temperature of 0 K of NEMS. Another important result is the prediction of the pull-in instability, corresponding to the on–off transition of the device, a key design parameter for NEMS.

Some interesting experimental observations of free thermal vibrations for singly and doubly clamped nanotubes were reported, respectively, by Chopra and Zettl [24] and Babic *et al.* [25]. For the cantilever nanotube, $E \approx 1.2$ TPa, $L \approx 154$ nm, $r = r_{\text{ext}} \approx 1.75$ nm, $r_{\text{int}} \approx 1.1$ nm ($M = \rho AL$, $J = \pi(r_{\text{ext}}^4 - r_{\text{int}}^4)/4$), and, according to Eq. (16), the amplitude of the thermal vibrations at 300 K of the free end is estimated to be on the order of ~1.4 nm; the root-mean-square amplitude (obtained by dividing for $\sqrt{2}$) is consequently on the order of 1 nm, close to the observed value of ~0.8 nm. On the other hand, the frequency ($P^{-1} = \omega/(2\pi)$), according to Eq. (13), is estimated to be on the order of ~0.4 GHz. Finally, the vibrations at a temperature of 0 K, according to Eq. (24), are estimated to have an amplitude on the order of ~0.05 Å.

For the clamped–clamped nanotube, $E \approx 1$ TPa, $L \approx 6.25$ μm, $r = r_{\text{ext}} \approx 1$ nm, $r_{\text{int}} \approx 0.665$ nm, and, according to Eq. (16), the amplitude of the thermal vibrations at 300 K of the free end is estimated to be on the order of ~0.13 μm (rms), close to the observed value of ~0.08 μm. The frequency, according to Eq. (13), is estimated to be on the order of ~0.7 MHz. Finally, the vibrations at a temperature of 0 K, according to Eq. (24), should have an amplitude on the order of ~0.2 Å (note that these comparisons simply assume the reported rough estimations for the parameters α, β, and $\rho_m = 2260$ kg/m^3; better estimations could be obtained considering more realistic forms for $w_S(s)$; in addition, strictly speaking, the parameters k, ζ should be considered experimental or numerical quantities).

Table 1. Comparison between theoretical and numerical predictions for pull-in voltages of nanotube-based NEMS

Case	H, nm	L, nm	$r = r_{ext}$, nm	r_{int}, nm	E, TPa	V_{PI}, V (theor.)	V_{PI}, V (calcd.)
1	100	2000	9.015	6	1	1.44	1.42
2	600	2000	9.015	6	1	13.56	13.40
3	1200	2000	9.015	6	1	30.89	30.52
4	100	4000	9.015	6	1	0.37	0.37
5	600	4000	9.015	6	1	3.39	3.35
6	1200	4000	9.015	6	1	7.72	7.63

Since no extensive investigations on the dynamics of NEMS under external fields are present in the literature, an additional possible check of the analysis can be achieved by comparing the prediction of the instability with a linear numerical analysis [23], for which E = 1.2 TPa, $r_{int} = 0$ nm, $L = 50$ nm, $r = 1$ nm, $H = 4$ nm. The comparison is reported in Table 1 by varying the length and the gap of the NEMS and, thus, its characteristic horizontal and vertical sizes. We conclude that the theory and numerical results agree satisfactorily, confirming the value of $k \approx 0.85$ for nanotubes.

ACTIVE CURRENT AND VOLTAGE CONTROLS

Voltage and current control. According to the previous analysis, we assume here $Z = 0$. As a consequence of the applied voltage, the nanotube will be deformed and its tip will have a vertical displacement c towards the electrode, as was previously discussed. The tunneling current arises between the nanotube tip and the electrode for a small gap $a = H - c$ (with a, we simply denote here the gap tip). A similar effect could arise as a consequence of the field emission also for larger gaps. Let us focus on nanotubes, even if a similar analysis could be applied to nanowires.

The resistance of the tunneling contact can be described as a function of the tip gap a as [3]

$$R_T(a) = R_0 e^{\frac{a}{\lambda}}, \tag{31}$$

where R_0 is the contact resistance between the nanotube and the electrode (valuable experimentally [19]) and λ is a material constant defined as $\lambda^{-1} = \sigma\sqrt{\Phi}$, where σ is a constant ($\sigma \approx \frac{1}{\text{Å}\sqrt{\text{eV}}}$ [20]) and Φ is the work function of the nanotube. For multiwalled nanotubes, $\Phi \cong 5$ eV [21]; thus, $\lambda^{-1} \cong 2.28$ Å$^{-1} \cong 22.8$ nm^{-1}. Accordingly, the tunneling current is given by $I(a) = \frac{V(a)}{R_T(a)}$. The function $V(a)$ describes the equilibrium positions of the nanotube tip under the voltage V, as previously discussed. In particular, by minimizing the free energy of the NEMS (Eq. (25)), we obtain

$$V(c) \approx 0.95 S\left(\frac{c}{H}\right) V_{PI}, \text{ where}$$
$$S\left(\frac{c}{H}\right) \approx \left\{ \sum_{i=0}^{\infty} \frac{1}{(2i+3)} \left(\frac{c}{H}\right)^{i-1} \right\}^{-\frac{1}{2}}, \tag{32}$$

where V_{PI} is given by Eq. (28) and $(c/H)_{PI} \approx 2/3$. Since $a = H - c$, it is clear that Eq. (32) represents an estimate for the function $V(a)$, i.e., the voltage–displacement electromechanical characteristic curve. Note that the curve of Eq. (32), like the pull-in voltage given by Eq. (28), agrees very well with numerical [22] and experimental [9] results.

For ease of representation of the electromechanical characteristic curves, the main parameters of the model are expressed as dimensionless functions or variables by the following normalization:

$$I^*(a) = \frac{V^*(a)}{R^*(a)}, \quad R^* = \frac{R_T}{R_0}, \quad I^* = \frac{I}{I_0},$$
$$I_0 = \frac{V_{PI}}{R_0}, \quad V^* = \frac{V}{V_{PI}}. \tag{33}$$

Since Eq. (32) represents the voltage–displacement characteristic curve and Eq. (33) represents the voltage–current characteristic curve, the current–displacement electromechanical characteristic curve is easily derived by combining them.

The displacement–voltage characteristic curve of the device is reported in Fig. 2. If the voltage is controlled (by introducing an ideal voltage source in series with the nanotube; see Fig. 1 with $Z = 0$), the pull-in instability will arise at the maximum of the curve, since the voltage does not increase monotonically with the displacement. On the other hand, the displacement–current characteristic curve of the device is reported in Fig. 3, plotted as an example for the case of $H = 10$ nm (H is the only parameter that has to be specified in such a dimensionless curve). If the current is controlled (by introducing an ideal current source in series with the nanotube; see Fig. 1 with $Z = 0$), the pull-in instability disappears, since the current monotonically increases

by increasing the displacement; this characteristic shows that imposing a current results in fixing the tip position, so that active control is achieved. Finally, in Fig. 4, the voltage–current characteristic of the device (H = 10 nm) is depicted.

In summary, if the device is directly voltage-controlled, according to our analysis, the pull-in will arise at a given value of the applied voltage as predicted by Eq. (28), namely, at the maximum of the curve reported in Fig. 2. The descending branch is unstable, since the voltage does not increase monotonically with an increase in the tip displacement. If we control the device in current, the entire curve reported in Fig. 2 represents stable configurations, as suggested by Fig. 3; this shows that a given tip position c corresponds to a given current $I(c)$ and vice versa. This is the main reason that the current control is stable everywhere. Consequently, the ideal current control results in an active analogical NEMS device. This nontrivial result shows that, by "simply" controlling the current in the picoampere regime (by an ideal current source), the displacement of the tip of the nanotube is actively controlled.

The role of the impedance Z. As previously discussed, the current control can be considered "active" even for negligible impedance Z. In contrast, due to the instability in the descending branch of Fig. 2, the voltage control has to be optimized. Here, we show that an active voltage control can be achieved considering an impedance Z in the circuit. If $Z = 0$, the pull-in of the device will take place by increasing the voltage; in this case, to reach the pull-out of the device, we have to consider a third ground element to impose charges of the same sign in both the nanotube and the electrode [11]. Recently, Kinaret *et al.* [12] have demonstrated that, for the voltage control case, tunneling between the tip of the nanotube and the electrode may cause the pull-out of the device. In [17, 18], a feedback control NEMS by employing a resistor R_F in series with the resistance of the tunneling contact is proposed. We discuss here analytically their numerical study. The control is achieved by imposing an input voltage U different from the voltage drop V on the nanotube, as discussed in the Introduction. For an active voltage control, U has to increase monotonically when the nanotube approaches the contact. This is the role of the impedance Z. This additional element is demonstrated to be sufficient to reach a new stable position just before the contact.

Let us consider the NEMS device described in Fig. 1, in which we have a voltage source delivering a voltage U, a resistance $Z = R_F$ in series with the cantilever nanotube, and the tunneling resistance R_T. Without current in the circuit, the voltage drop on the nanotube-bottom electrode gap is $V = U$. Once established, the tunneling current will reduce the voltage V between the nanotube and electrode, according to the partition of voltage, in the dimensionless form

$$V^{**}(a) = \frac{V(a)}{U} = \frac{R^{**}(a)}{1 + R^{**}(a)}, \quad R^{**} = \frac{R_T}{R_F}, \quad (34)$$

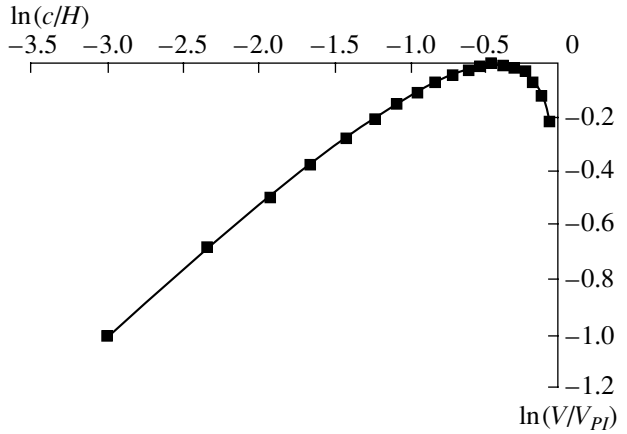

Fig. 2. Displacement–voltage electromechanical characteristic curve (voltage control: the pull-in instability arises at the maximum of the curve).

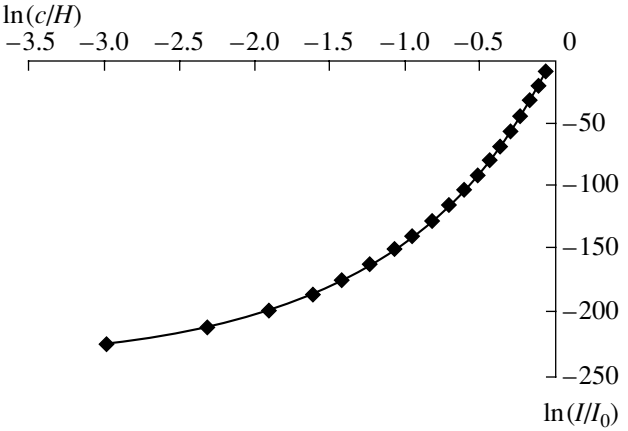

Fig. 3. Displacement–current electromechanical characteristic curve (current control: the pull-in instability disappears; H = 10 nm).

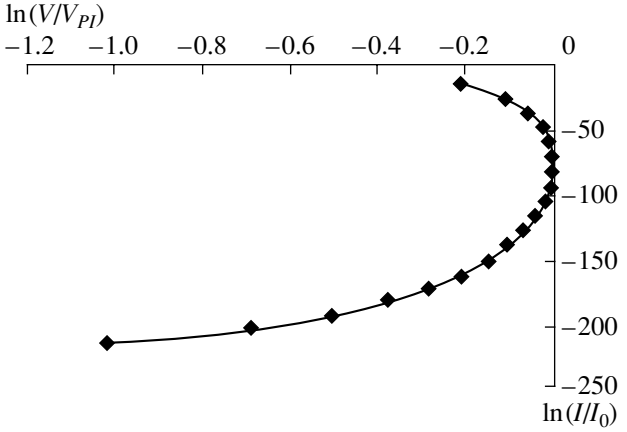

Fig. 4. Voltage–current characteristic curve (H = 10 nm).

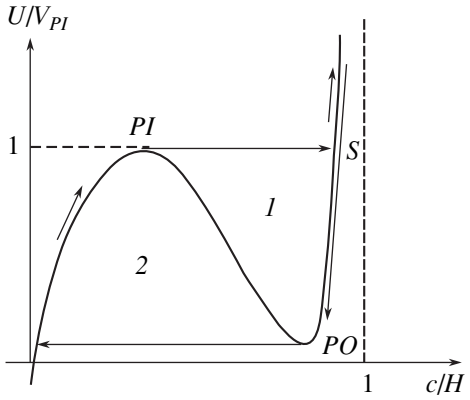

Fig. 5. Displacement–voltage characteristic (qualitative) curve with an impedance Z in the circuit.

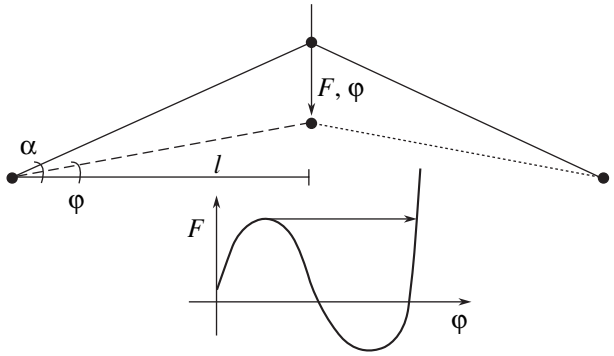

Fig. 6. Mechanical analogy of NEMS controls. Force control corresponds to voltage control; displacement control corresponds to current control.

where R_T is given by Eq. (31). The decrease in the voltage V with the gap a via $R_T(a)$ causes a reduction in the deflection of the nanotube, and practically a new stable second position will be reached after the pull-in voltage and before the contact. The phenomenon is qualitatively illustrated in Fig. 5. For a "moderate," e.g., around 10 nm, distance between the nanotube and the electrode, this curve coincides with the characteristic curve reported in Fig. 2. For very small electrode–nanotube tip distances (~1 nm), the tunneling current will be established, decreasing the voltage V, so that the nanotube will reach a second stable equilibrium position. As a consequence, an ascending branch will be present in the characteristic curve. Assuming an increase in the voltage U, the device will follow the marked ascending path, reaching the pull-in at the point *PI* and, just before the contact, a stable position at the point *S*. From here, when the source voltage U is increased, the nanotube will approach the electrode. On the other hand, if U is decreased, the device will follow the marked descending path to reach the pull-out in *PO*. The areas denoted by *1* and *2* are proportional to the square root of the kinetic energies released in the corresponding two instabilities that will be dissipated as a consequence of the damping of the system.

A mechanical analogy could be represented by the snap-through in the system reported in Fig. 6 (opposite elastic beams of length l inclined by an angle α and with stiffness Q). Controlling the force F (analogous to controlling U) causes an increase in the angular displacement φ and a collapse (snap-through, analog to the pull-in) before reaching the horizontal configuration. The elastic energy thus released is converted into kinetic energy. If a dissipative element exists, the system will reach a new stable equilibrium condition, thanks to the presence of the internal hinge (playing the role of the two resistances). Controlling the displacement (analogous to controlling the current), all of the configurations are stable. Obviously, the analogy is not complete, as emphasized by the qualitative equilibrium force versus displacement curve reported in Fig. 6. As in the previous treatment, such a characteristic can be obtained with respect to the angle φ, the free energy of the system here given by $W = Q\left(\frac{l}{\cos\alpha} - \frac{l}{\cos(\alpha-\varphi)}\right)^2 - Fl(\tan\alpha - \tan(\alpha-\varphi))$, assuming small angles.

Second equilibrium position. To estimate the second equilibrium position of the NEMS, we present here a simplified approach; a corresponding numerical investigation was performed in [17, 18]. Approaching the contact, the predominant contributions in the forces are the singular terms, i.e., the electrostatic, the van der Waals, and the Pauli forces. Accordingly, the equilibrium, as a first approximation, can be written considering the forces per unit length q evaluated at the tip (singular contributions):

$$\frac{d}{da}\left\{\frac{\partial\varepsilon_{\text{elec}}}{\partial z}(a) + \frac{\partial\varepsilon_{vdW}}{\partial z}(a) + \frac{\partial\varepsilon_{\text{Pauli}}}{\partial z}(a)\right\} = 0. \quad (35)$$

The derivation of the first term in Eq. (35) generates two terms: the first one, q_{elec}, is present as a consequence of the variability of the capacitance per unit length of the nanotube with respect to the gap a; the second one, $q_{\underset{\text{tun}}{\text{elec}}}(a)$, represents a new (tunneling) term, as a consequence of the fact that, here, the voltage V is not imposed but is itself a function of the gap a; i.e., $V(a)$. Note that Eq. (35) represents a balance of singular forces (per unit length, evaluated around the tip); i.e., $q_{\text{elec}}(a) + q_{\underset{\text{tun}}{\text{elec}}}(a), + q_{vdW}(a) + q_{\text{Pauli}}(a) = 0$.

To obtain a simple estimation, we model the van der Waals and Pauli forces as a mechanical contact [12] at $a = a_{\min} \approx 0.35$ nm. Correspondingly, before the mechanical contact $q_{vdW} \approx 0$ and $q_{\text{Pauli}} \approx 0$, so that

Eq. (35) reduces to $q_{\underset{\text{tun}}{\text{elec}}}(a) + q_{\text{elec}}(a) \cong 0$. Noting that $\frac{\partial \varepsilon_{\text{elec}}}{\partial z} = \frac{\pi\varepsilon_0 V(a)^2}{\cosh^{-1}\left(1+\frac{a}{r}\right)}$, we obtain the two terms as

$$q_{\text{elec}} = \frac{\pi\varepsilon_0 V^2}{\sqrt{a(a+2r)}\log^2\left(1+\frac{a}{r}+\frac{\sqrt{a(a+2r)}}{r}\right)},$$
$$q_{\underset{\text{tun}}{\text{elec}}} = -\frac{2\pi\varepsilon_0 V^2}{\lambda(1+R^{**})\cosh^{-1}\left(1+\frac{a}{r}\right)}. \quad (36)$$

Considering the asymptotic behavior of Eq. (36) for $a/r \longrightarrow 0$ yields

$$q_{\text{elec}} \cong \frac{\pi\varepsilon_0 V^2}{\sqrt{2ar}\frac{2a}{r}}, \quad q_{\underset{\text{tun}}{\text{elec}}} \cong -\frac{2\pi\varepsilon_0 V^2}{\lambda(1+R^{**})\sqrt{\frac{2a}{r}}} \quad (37)$$

and, consequently, the equilibrium $q_{\text{elec}}(a) + q_{\underset{\text{tun}}{\text{elec}}}(a) \cong 0$ gives

$$4\frac{a}{\lambda} - \frac{R_0}{R_F}e^{\frac{a}{\lambda}} - 1 = 0. \quad (38)$$

Note that a/λ is of the order of 20, and, consequently, $e^{a/\lambda}$ cannot be approximated considering small values of a/λ. The solution of Eq. (38) defines the value of a corresponding to the second stable equilibrium position after the pull-in due to the tunneling effect. Analysis shows that it is only slightly dependent on R_0/R_F; the dependence on this parameter is clear: as expected, the lower the ratio R_0/R_F, the larger the tip gap corresponding to the tunneling equilibrium. Approximate Eq. (38) suggests also that the equilibrium position is practically independent of the applied voltage U. Accordingly, such an equilibrium position is theoretically expected to be very stable. The corresponding tunneling current is given by $I(a) = \frac{V(a)}{R_T(a)}$.

Solving Eq. (38), the equilibrium positions corresponding to gaps of the order of 0.5–1 nm have been found by varying R_0/R_F within four orders of magnitude (see Table 2). The corresponding tunneling currents are also estimated (Table 2). Note that the large variation in the tunneling current for a small variation of the tip position suggests that the current control previously proposed (if close to "ideal") could result in a high positioning accuracy. Decreasing the voltage U, the pull-out of the device will arise for a small value of U_{PO}/V_{PI}. According to simplified hypotheses, the equilibrium positions reported in Table 2 can be considered to be only estimates. Numerical investigations performed as described in [17, 18], including van der Waals forces and charge tip concentration (but still neglecting the Pauli principle), basically confirm this trend (Table 2).

Table 2. Second stable equilibrium position: theoretical estimations (and corresponding tunneling currents) and numerical predictions. The numerical result yielding an equilibrium of a gap lower than 0.4 nm is not attainable, since, in this range, the Pauli principle cannot be neglected

$\frac{R_F}{R_0}$	I, pA (theor.)	a, nm (theor.)	a, nm (calcd.)
10^5	86.95	0.68	<0.4
10^6	7.48	0.79	0.49
10^7	0.66	0.89	0.61
10^8	0.06	1.00	0.72

CONCLUSIONS

In this paper, nanotube- and nanowire-based NEMS have been investigated. The frequency and amplitude of the vibrations (free, thermal, and as imposed by the uncertainty principle, including the electric field and van der Waals forces), as well as the instability corresponding to the switch of the device are quantified by the proposed free-energy-based approach. Two different types of control, thanks to the tunneling current, have been demonstrated to allow the realization of digital (voltage control) as well as analogic (current control) devices. The electromechanical characteristics of the NEMS have been deduced.

ACKNOWLEDGMENTS

The author would like to acknowledge A. Carpinteri, H.D. Espinosa, C.H. Ke, and N. Moldovan for discussions and to Diane Dijak for the English grammar supervision.

REFERENCES

1. Yang, Y.T., Ekinci, K.L., Huang, X.M.H., *et al.*, Monocrystalline Silicon Carbide Nanoelectromechanical Systems, *Appl. Phys. Lett.*, 2001, vol. 78, pp. 162–164.
2. Cleland, A.N. and Roukes, M.L., Fabrication of High-Frequency Nanometer-Scale Mechanical Resonators from Bulk Si Crystals, *Appl. Phys. Lett.*, 1996, vol. 69, pp. 2653–2655.
3. Erbe, A., Blick, R.H., Tilke, A., Kriele, A., and Kotthaus, P., A Mechanical Flexible Tunneling Contact Operating at Radio Frequency, *Appl. Phys. Lett.*, 1998, vol. 73, pp. 3751–3753.
4. Huang, X.M.H., Zorman, C.A., Mehregany, M., and Roukes, M.L., Nanodevice Motion at Microwave Frequencies, *Nature* (London), 2003, vol. 421, p. 496.

5. Roukes, M.L., Nanoelectromechanical System, *Technical Digest of the 2000 Solid-State Sensor and Actuator Workshop*, 2000.
6. Abadal, G., Davis, Z.J., Helbo, B., *et al.*, Electromechanical Model of a Resonating Nano-Cantilever-Based Sensor for High-Resolution and High-Sensitivity Mass Detection, *Nanotechnology*, 2001, vol. 12, pp. 100–104.
7. Martel, R., Schmidt, T., Shea, H.R., Hertel, T., and Avouris, Ph., Single- and Multi-Wall Carbon Nanotube Field-Effect Transistors, *Appl. Phys. Lett.*, 1998, vol. 73, pp. 2447–2449.
8. Cleland, A.N. and Roukes, M.L., A Nanometer-Scale Mechanical Electrometer, *Nature* (London), 1998, vol. 392, pp. 160–162.
9. Akita, S., Nakayama, Y., Mizooka, S., *et al.*, Nanotweezers Consisting of Carbon Nanotubes Operating in an Atomic-Force Microscope, *Appl. Phys. Lett.*, 2001, vol. 79, pp. 1691–1693.
10. Kim, P. and Lieber, C.M., Nanotube Nanotweezers, *Science* (Washington, D. C., 1883–), 1999, vol. 126, pp. 2148–2150.
11. Rueckes, T., Kim, K., Joslevich, E., *et al.*, Carbon Nanotube-Based Nonvolatile Random Access Memory for Molecular Computing, *Science* (Washington, D. C., 1883–), 2000, vol. 289, pp. 94–97.
12. Kinaret, J., Nord, T., and Viefers, S., A Carbon-Nanotube-Based Nanorelay, *Appl. Phys. Lett.*, 2003, vol. 82, pp. 1287–1289.
13. Fennlmore, A.M., Yuzvlnsky, T.D., Han, W.Q., *et al.*, Rotational Actuator Based on Carbon Nanotubes, *Nature* (London), 2003, vol. 424, pp. 408–410.
14. Pugno, N. and Ruoff, R., Quantized Fracture Mechanics, *Philos. Mag.*, 2004, vol. 84, no. 27, pp. 2829–2845.
15. Pugno, N., Non-Linear Dynamics of Nanotube Based NEMS, in *Recent Research Developments in Sound and Vibrations*, Transworld Research Network, 2004, vol. 2, pp. 197–211.
16. Pugno, N., Dynamics of Nanotube Based NEMS, in *Proceedings of XI International Congress on Sound and Vibrations, St. Petersburg. Russia, July 5–8, 2004*, CD-ROM (no. 283).
17. Ke, C-H., Espinosa, H.D., and Pugno, N., A Feedback Controlled Carbon Nanotube Based NEMS Device, in *Proceedings of International Conference on Experimental Mechanics-12, Bari, Italy, August 29–September 2, 2004*, CD-ROM (no. 81).
18. Ke, C.H. and Espinosa, H.D., A Feedback Controlled Nanocantilever NEMS Device, *Appl. Phys. Lett.*, 2004 (in press).
19. Tarkiainen, R., Ahlskog, M., Penttila, J., *et al.*, Multiwalled Carbon Nanotube: Luttinger versus Fermi Liquid, *Phys. Rev. B: Condens. Matter*, 2001, vol. 64, p. 195412.
20. Stroscio, J.A., *et al.*, Scanning Tunneling Microscopy, *Methods of Experimental Physics,* Boston: Academic, 1993, vol. 27.
21. Sun, J.P., Work Function of Single-Walled Carbon Nanotubes Determined by Field Emission Microscopy, *Appl. Phys. A,* 2002, vol. 75, pp. 479–483.
22. Dequesnes, M., Rotkin, S.V., and Aluru, N.R., Calculation of Pull-in Voltage for Carbon-Nanotube–Based Nanoelectromechanical Switches, *Nanotechnology*, 2002, vol. 13, pp. 120–131.
23. Ke, C.H., Espinosa, H.D., and Pugno, N., Analysis of Nanotubes Based NEMS Devices: Role of Finite Kinematics, Stretching and Charge Concentrations, *J. Appl. Mech.* (in press).
24. Chopra, N.G. and Zettl, A., Measurement of the Elasticity of a Multi-Wall Boron Nitride Nanotube, *Solid State Commun.*, 1998, vol. 105, pp. 297–300.
25. Babic, B., Furer, J., Sahoo, S., Farhangfar, Sh., and Schonenberger, C., Intrinsic Thermal Vibrations of Suspended Doubly Clamped Single-Wall Carbon Nanotubes, *Nanoletters*, 2003, vol. 3, pp. 1577–1580.